Correlation between Charge State of Insulating NaCl Surfaces and Ionic Mobility Induced by Water Adsorption: A Combined Ambient Pressure X-ray Photoelectron Spectroscopy and Scanning Force Microscopy Study

Albert Verdaguer,*,† Juan Jose´ Segura,† Jordi Fraxedas,† Hendrik Bluhm,‡ and Miquel Salmeron‡,§

Centre d Investigacio´ en Nanocie´ncia i Nanotecnologia, CIN2 (CSIC-ICN), Esfera UAB, Campus de la UAB, Edifici CM-7, 08193-Bellaterra, Catalunya, Spain; Lawrence Berkeley National Laboratory, Berkeley, California 94720; and Materials Science and Engineering Department, University of California, Berkeley, California 94720

* Corresponding author. E-mail: Albert.Verdaguer.ICN@uab.cat.

† CIN2 (CSIC-ICN).

‡ Lawrence Berkeley National Laboratory.

§ University of California, Berkeley.

In situ ambient pressure X-ray photoelectron spectroscopy (APPES) and scanning force microscopy were used to characterize the surface discharge induced by water layers grown on (001) surfaces of sodium chloride single crystals. The APPES studies show that both kinetic energy (KE) and full width at half-maximum (FWHM) of the Na 2s and Cl 2p core level peaks, monitored as a function of relative humidity (RH), mimic surface conductivity curves measured using scanning force microscopy. The KE position and FWHM of the core level peaks therefore are directly related to the solvation and diffusion of ions at the NaCl(100) surface upon adsorption of water.

I. Introduction

Over the past four decades experimental strategies have been developed to extend the pressure range of X-ray photoelectron spectroscopy (PES) from ultrahigh vacuum (UHV) to the Torr range, in order to characterize liquid/vapor and solid/vapor interfaces under realistic (ambient) conditions of temperature and pressure.[1-3] Pressures higher than 5 Torr are of particular importance for environmental science because the vapor pressure of water at the triple point, where gas, liquid, and solids phases coexist in thermodynamic equilibrium, is 4.6 Torr at 273 K. The principal obstacle encountered with PES at elevated pressures is the intrinsic limited mean free path of electrons through gases, with an approximate value of 1 mm at a KE of 100 eV in 1 Torr of water vapor.[4] Ambient pressure X-ray photoelectron spectroscopy (APPES), a recent modification of the PES technique, overcomes this obstacle by means of differential pumping stages, where the sample is placed very close (~1 mm) to the entrance aperture of a differentially pumped electrostatic lens system, thereby limiting the path length of the electrons in the high-pressure region while keeping the electron detector in UHV. APPES has enabled the study at realistic operating pressures of liquid/vapor and solid/vapor interfaces that are important for catalysis,[5-7] atmospheric chemistry,[8] and the interaction of water with solid surfaces.[9] In this work we show that surface charging, a common hindrance in photoemission experiments on insulating samples, can be used to obtain information about the properties of solid/ vapor interfaces, in particular their surface conductivity. We show how the surface of NaCl discharges upon water adsorption, as measured by a combination of APPES and Kelvin probe microscopy (KPM).

II. Experimental Section

The APPES measurements were carried out at beamline 11.0.2 of the Advanced Light Source at Lawrence Berkeley National Laboratory, using a photoelectron spectrometer with a three-stage differentially pumped electrostatic lens system, which allows measurements at background pressures of up to 10 Torr.[3] Photoemission spectra of the Cl 2p and Na 2s core levels were recorded using incident photon energies of 335 and 195 eV, respectively. In this way photoelectrons for both core levels have similar KEs, ~125 eV, ensuring a similar probing depth for both elements and high surface sensitivity. In addition, O 1s and C 1s core levels were also recorded in order to track the adsorption of water layers and to control the level of contamination of the sample,

respectively. The results were found to be independent of the small amount (submonolayer coverage) of carbonaceous materials, which are present as contaminants and whose concentration varies from surface to surface. The sample position was changed between acquisitions of each series of spectra to minimize beam damage. Cleaved synthetic NaCl(001) single crystals (MaTeck GmbH, Ju¨lich, Germany, 99.999% purity) were mounted on cooled/ heated copper holders electrically grounded. Cleavage was performed either in situ, at a base pressure of ~10-7 Torr, or ex situ just before introduction into the vacuum system (ambient RH < 35%). Vapor from degassed high-performance liquid chromatography (HPLC) grade water was introduced through a leak valve, and its pressure was monitored with a capacitance manometer gauge. The water vapor pressure in the chamber was kept constant (2 Torr), and the sample temperature (T_s) was varied to control the RH. We estimate the RH (in %) in the area near the sample from the ratio between the fixed 2 Torr pressure and the saturated water vapor pressure at thesample temperature. KPM images were taken at room temperature (21 (1 °C) with a home-built AFM[10] and a commercial SPM100 electronic control from RHK Technology, Inc.. Images were taken in the scanning polarization force microscopy (SPFM) mode.[11] The microscope head was enclosed in a glovebox. Humidity control was achieved by circulating dry N_2 to decrease RH or by bubbling N_2 through deionized water to increase RH. RH was measured using an Omega hygrometer. The absolute RH values have an uncertainly of (5%.).

III. Results

Figure 1 shows the experimental KE ~ 125 eV Cl 2p (top) and Na 2s (bottom) PES core levels measured at 5% (T_s) 34.2 °C) and 65% (T_s) -5.4 °C) RH, respectively, together with least-squares fit Voigt functions after a Shirley-type background subtraction. The fits have been performed with single components, one for Na 2s and a single spin-orbit doublet for Cl 2p, so that within the experimental error only one type of species at the surface is observed in the whole RH range. In both cases we observe an obvious decrease of the FWHM and an increase in KE for increasing RH. The same behavior was observed in additional experiments performed at higher KEs (see Figure S1 in Supporting Information).

In Figure 2 we summarize the RH dependence of both KE (top) and FWHM (bottom) for the Cl 2p line (KE ~ 125 eV). Both curves show distinct regions, which we label A, B, C, and D. Region A, from the lowest humidity to ~20% RH (T_s) 11.3 °C), exhibits a small increase in KE (~0.3 eV) until reaching an intermediate stable value at 30-35% RH (region B). Above 35% RH (T_s) 2.9 °C) a clear increase in KE is observed up to 50% RH (region C). Finally, above 55% RH (region D, T_s) -3.0 °C) the KE value remains unchanged. The total KE shift is 3 eV for Cl 2p. The same overall behavior is observed for the Na 2s line, as shown in the upper part of Figure 3, although in this case the total shift is smaller (2.5 eV). This effect might be related to the different susceptibility of Na and Cl to beam damage. Chlorine ions tend to desorb or diffuse under the influence of soft X-ray photons, a process that should enhance water dissociation and formation of hydroxide ions, while sodium is less affected.[12,13] The results shown in Figures 2 and 3 have been obtained for increasing RH values. After reaching 65% RH, the RH was reduced to the initial 5% RH. The difference in KE at 5% RH (initial and final) is less than 0.5 eV, and in most cases less than 0.2 eV, thus showing only a slight hysteresis.

The FWHM curve (Figure 2, bottom curve) shows a similar dependence on RH. Region A exhibits a monotonous decrease of FWHM, up to 80% of the original value. In region B the FWHM of Cl 2p peak remains approximately constant, until it starts to decrease rapidly at about 35% RH, eventually reaching a value of 1 eV (~60% of the initial FWHM) at ~50% RH (region C). An increase in the RH from this point on does not lead to a further decrease in the FWHM value, and it oscillates around 1 eV. In the case of the Na 2s spectra (Figure 3, bottom curve) a similar trend can be observed with a final FWHM reduced to ~65% of the initial value at 65% RH.

IV. Discussion

The positive shift of KE for increasing RH values is due to global discharging of the surface.[14] Below the onset of strong discharging at 35% RH, the insulating surface becomes slightly discharged due to the combined effect of the ionized water vapor, secondary electrons, and generation of charge carriers (i.e., color centers) induced by photons. Discharging becomes more efficient once surface ions become mobile due to salvation after water adsorption. Ion mobility allows the discharging of the surface through the grounded copper holder. Ionic

conductivity measurements of NaCl crystals as a function of RH revealed the existence of two different regimes above and below a characteristic RH value of ~40%, close to our 35% value.[15] This characteristic RH has been also related, according to scanning force microscopy studies, to the beginning of largescale modifications of the surface step structure due to ion mobility on the surface.[16] In addition, infrared studies showed that this change is associated with a sudden increase of water coverage at ~40% RH from submonolayer coverage to ~3 monolayers.[17,18] Below this characteristic RH, ion mobility was observed but mostly limited to step sites.[11] In the top parts of Figures 2 and 3 we observe that the main KE shift happens in region C around this critical RH, indicating that surface ion mobility is contributing to the discharging of the sample surface. Above about 50% RH the surface seems to be effectively discharged, given that the KE of the core levels remains essentially constant.

KPM measurements have shown that the mean surface potential value of a NaCl(001) surface changes when exposed to water.[11] A change in the surface potential would induce a shift in the peak position if the sample surface is floating and does not have any electrical connection to ground as it is for our NaCl surface before adsorbed water allows surface ion mobility. However, this variation was found to be ~0.25 V in the RH range of our experiments,[19] thus insufficient to explain our ~2.5-3 eV KE shift.

Let us now comment on the closely related evolution of the FWHM. In the low-RH region (region A) the FWHM drops significantly before reaching the plateau corresponding to region B (see bottom curves of Figures 2 and 3). This effect is more evident than the corresponding small KE shift. We attribute this behavior mainly to the reduction of inhomogeneities in the surface potential of the NaCl(001) surface, which were observed in KPM studies of freshly cleaved NaCl(100) surfaces at low RH. Inhomogeneities of the surface potential are mainly produced by a surface potential difference between the steps and the terraces. However, many inhomogeneities can be also observed within the terraces, as illustrated with the KPM image in Figure 2 at region A. Such inhomogeneities at terraces, mainly due to surface charged defects caused by cleavage, were found to have differences in surface potential as large as 0.2 V.[11] They disappear as soon as water adsorbs on the surface, and at ~25% RH only differences between steps and terraces can be observed (see KPM image in Figure 2 at region B). The surface potential inhomogeneities induce a dispersion of the KE values of the photoelectrons generated at different locations of the surface, leading to peak broadening. The FWHM decay in this first region is ~0.3 eV for the Cl 2p and 0.2 eV for the Na 1s, thus of the order of surface potential differences observed by KPM.

The surface potential differences between steps and terraces at 30% RH are ~0.1 V.[11] These differences are strongly reduced between 35 and 50% RH, and above 50% KPM images show no appreciable differences and a homogeneous surface potential distribution (see KPM image in Figure 2, regions C and D). The region where this decay shows up corresponds to the region where FWHM also shows its larger decay. This decay was found to be ~0.3 eV for the Cl 2p and 0.2 eV for the Na 2s, larger than the 0.1 V referred above, indicating the dominant contribution from discharge in region C. The limiting FWHM values achieved above 50% RH, 1.0 and 1.3 eV for Cl 2p and Na 2s, respectively, are essentially due to phonon broadening (Franck-Condon principle).[20] The calculated phonon contribution to the width is 0.75 eV.[21] In addition, one should add the combined analyzer-monochromator resolution, which is better than 0.25 eV for both 195 and 335 eV photons, and the contribution from surface defects.[22] The limiting FWHM value of Na 2s is larger than that corresponding to Cl 2p due to Auger decay processes.

If we transform the FWHM vs RH curves into FWHM vs temperature curves, we obtain positive temperature coefficients of about 10 meV/K. Such a value is clearly larger than the estimated temperature coefficient for phonon broadening, which is about 1 meV/K, indicating the marginal contribution from phonon broadening to the observed FWHM variations (see Figure S2 in Supporting Information). The onset of ionic mobility-induced surface discharging to phonon broadening contributions to the FWHM has been observed for thin films of alkali halides, such as KF, measured with PES in ultrahigh vacuum, when heated above room temperature.[20]

In order to ascertain whether region C effectively corresponds to the growth of water layers, as suggested by infrared measurements, we focused on RHs around 40% and took Cl 2p, Na 2s, and O 1s spectra at small RH intervals. In Figure 4 we plot the measured KE values (left scale) of the Cl 2p peak together with the area of the O 1s peak from adsorbed water (see Figure S3 in Supporting Information). From the figure it can be observed

that from 32% to 42% both curves are roughly coincident, indicating that surface discharging through ionic mobility is correlated to the formation of a molecularly thin water layers.

V. Conclusions

APPES and KPM were used to characterize the surface discharge induced by water layers grown on (001) surfaces of sodium chloride single crystals. Photoelectron kinetic energies and peak widths of the Na 2s and Cl 2p core level peaks were monitored as a function of relative humidity. We have shown that changes in core level photoelectron kinetic energies and peak widths of insulating NaCl, which reflect variations in the charge state of the surface, are strongly correlated with important structural changes of the surface. These changes include ionic solvation and mobility, which occur first at step edges for $0 < RH < 35\%$, and step mobility and terrace ionic solvation for $RH > 35\%$. The discharge effects saturate at $RH > 50\%$ at the low frequency (dc) time scale of these experiments.

Acknowledgment. This work was supported by the Ministerio de Educacio´n y Ciencia (Spain), through project FIS2006- 12117-C04-01, by Generalitat de Catalunya (SGR 00909) and by the Director, Office of Science, Office of Biological and Environmental Research, the Materials Sciences Division and the Chemical Sciences Divisions of the U.S. Department of Energy, under Contract DE-AC02-05CH11231. A.V. acknowledges support from the Spanish Ramo´n y Cajal Program and the mobility BE program from Agaur, Generalitat de Catalunya. J.J.S. thanks the Consejo Superior de Investigaciones Cienti´ficas (CSIC) for a JAE DOC PhD grant.

Supporting Information Available: Evolution of the KE of the Cl 2p line excited with 735 eV photons vs RH (Figure S1), experimental values of the FWHM as a function of temperature (top curve) and calculated phonon contribution (bottom curve) according to ref 21 (Figure S2), and O 1s line spectrum showing the gas phase and adsorbed water contributions (Figure S3).

References and Notes

(1) Siegbahn, H.; Svensson, S.; Lundholm, M. *J. Electron Spectrosc.* **1981**, *24*, 205.
(2) Pantfo¨rder, J.; Po¨llmann, S.; Zhu, J. F.; Borgmann, D.; Denecke, R.; Steinru¨ck, H.-P. *ReV. Sci. Instrum.* **2005**, *76*, 014102.
(3) Ogletree, D. F.; Bluhm, H.; Lebedev, G.; Fadley, C. S.; Hussain, Z.; Salmeron, M. *ReV. Sci. Instrum.* **2002**, *73*, 3872.
(4) Redhead, P. A.; Hobson, J. P.; Kornelsen, E. V. *The Physical Basis of Ultrahigh Vacuum*; American Institute of Physics: New York, 1993.
(5) Ketteler, G.; Ogletree, D. F.; Bluhm, H.; Liu, H.; Hebenstreit, E. L. D.; Salmeron, M. *J. Am. Chem. Soc.* **2005**, *127*, 18269.
(6) Bluhm, H.; Ha¨vecker, M.; Knop-Gericke, A.; Kiskinova, M.; Schlo¨gl, R.; Salmeron, M. *MRS Bull.* **2007**, *32*, 1022.
(7) Blume, R.; Ha¨vecker, M.; Zafeiratos, S.; Teschner, D.; KnopGericke, A.; Schlo¨gl, R.; Dudin, P.; Barinov, A.; Kiskinova, M. *Catal. Today* **2007**, *124*, 71.
(8) Goshal, S.; Hemminger, J. C.; Bluhm, H.; Mun, B. S.; Hebenstreit, E. L. D.; Ketteler, G.; Ogletree, D. F.; Requejo, F. G.; Salmeron, M. *Science* **2005**, *307*, 563.
(9) Verdaguer Weiss, C.; Oncins, G.; Ketteler, G.; Bluhm, H.; Salmeron, M. *Langmuir* **2007**, *23*, 9699.
(10) Bluhm, H.; Pan, S. H.; Xu, L.; Inoue, T.; Ogletree, D. F.; Salmeron, M. *ReV. Sci. Instrum.* **1998**, *69*, 1781.
(11) Verdaguer, A.; Sacha, G. M.; Ogletree, D. F.; Salmeron, M. *J. Chem. Phys.* **2005**, *123*, 124703.
(12) Malaske, U.; Pfu¨r, H.; Ba¨ssler, M.; Weiss, M.; Umbach, E. *Phys. ReV. B* **1995**, *53*, 13115.
(13) Zielasek, V.; Hildebrandt, T.; Henzler, M. *Phys. ReV. B* **2000**, *62*, 2912.
(14) Citrin, P. H.; Thomas, T. D. *J. Chem. Phys.* **1972**, *57*, 4446.
(15) Hucher, M.; Oberlin, A.; Hocart, R. *Bull. Soc. Fr. Mineral. Cristallogr.* **1967**, *90*, 320.
(16) Dai, Q.; Hu, J.; Salmeron, M. *J. Phys. Chem. B* **1997**, *101*, 1994.
(17) Peters, S. J.; Ewing, G. E. *Langmuir* **1997**, *13*, 6345.
(18) Foster, M. C.; Ewing, G. E. *J. Chem. Phys.* **2000**, *112*, 6817.
(19) Cabrera-Sanfelix, P.; Sanchez-Portal, D.; Verdaguer, A.; Darling, G. R.; Salmeron, M.; Arnau, A. *J. Phys. Chem. C* **2007**, *111*, 8000.
(20) Citrin, P. H.; Eisenberger, P.; Hamann, D. R. *Phys. ReV. Lett.* **1974**, *33*, 965.
(21) Iwan, M.; Kunz, C. *Phys. Lett.* **1977**, *60A*, 345.
(22) Fraxedas, J.; Trodahl, J.; Gopalan, S.; Ley, L.; Cardona, M. *Phys.Rev. B* **1990**, *41*, 10068.

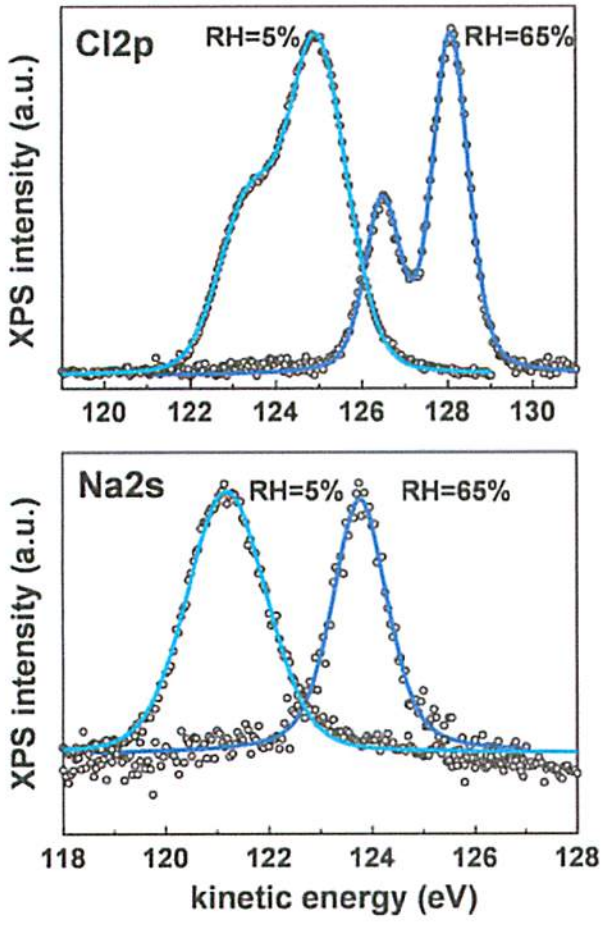

Figure 1. APPES spectra corresponding to the Cl 2p (top) and Na 2s (bottom) core levels measured at 5 and 65% RH, respectively, at 2 Torr water vapor pressure. The experimental data have been fitted to a Voigt function after a Shirley-type background subtraction. A single component has been used for Na 2s while for Cl 2p a single spin-orbit doublet with fixed spin-orbit splitting (1.6 eV) and branching ratio (0.5) and the same FWHM for both 3/2 and 1/2 components has been used.

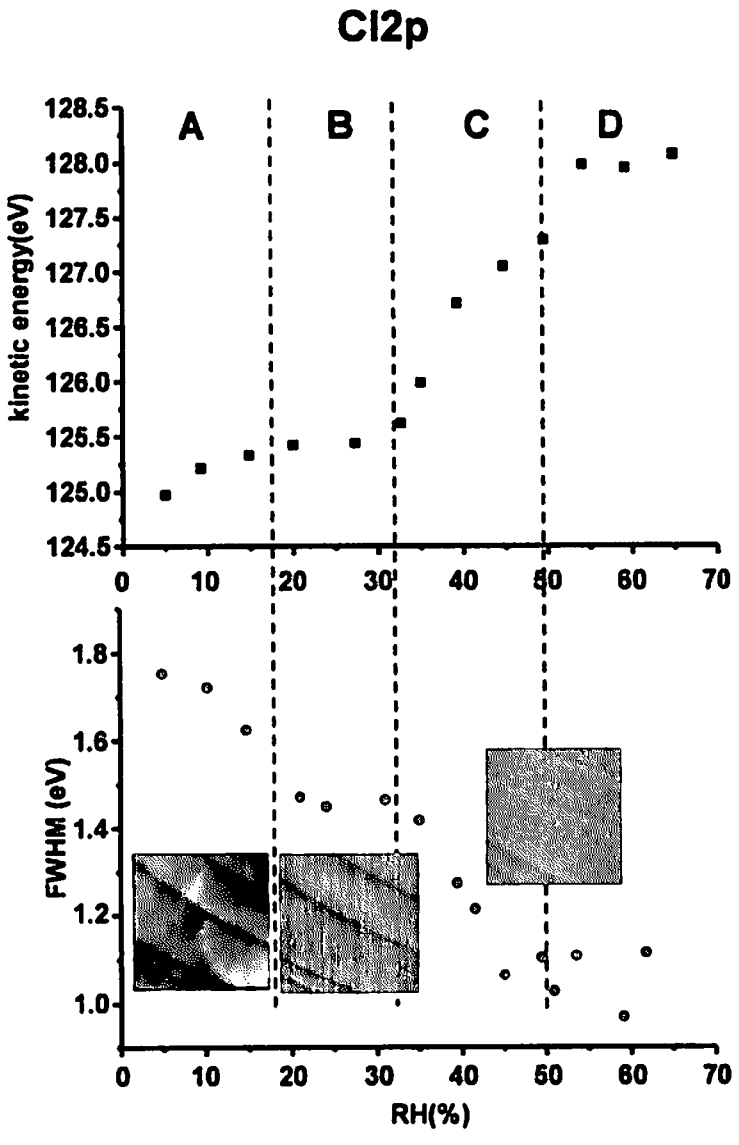

Figure 2. Evolution of the KE (top curve) and of the FWHM (bottom curve) of the Cl 2p line excited with 335 eV photons vs RH. Water vapor pressure was 2 Torr. The estimated errors in the KE and FWHM values are (0.2 and (0.1 eV, respectively. Also shown are 5 × 5 μm KPM images of a NaCl(001) surface taken with SPFM at different RH. Different regions (A, B, C, D) are defined according to the observed evolution of KE and FWHM with RH. These regions correspond to known important changes in the structure, contact potential, and ion mobility at the NaCl(001) surface as a function of RH.

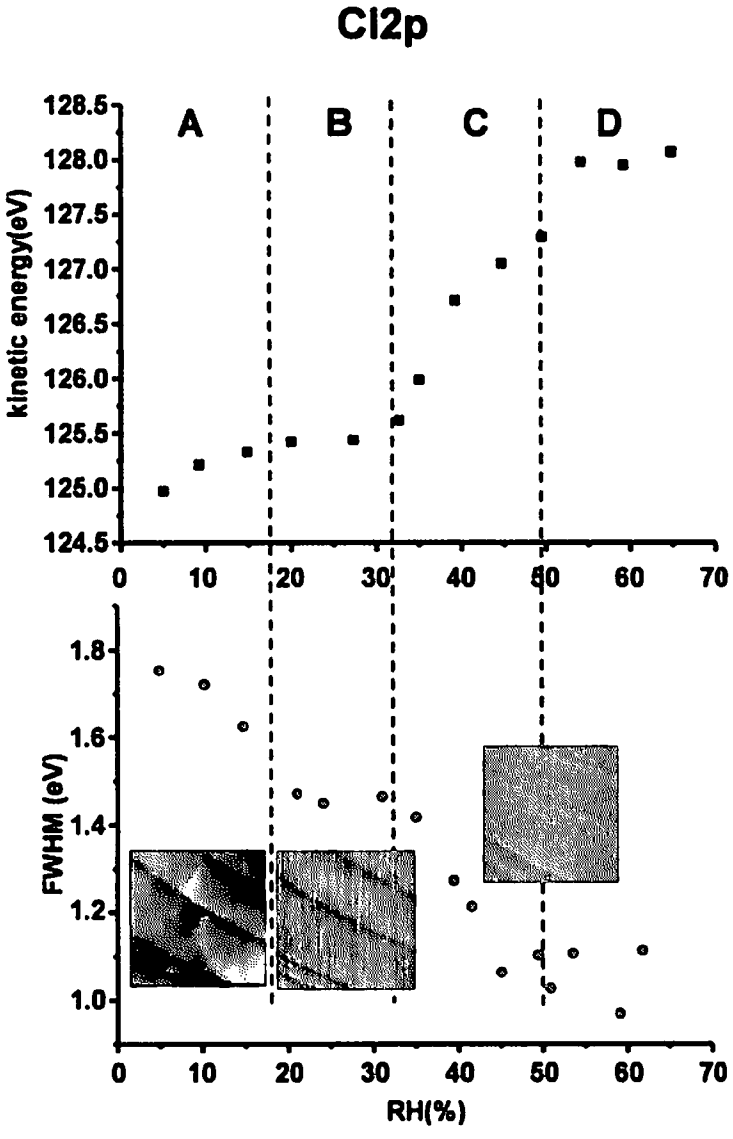

Figure 3. Evolution of the KE (top curve) and of the FWHM (bottom curve) of the Na 2s line excited with 335 eV photons vs RH. Water vapor pressure was 2 Torr. The estimated errors in the KE and FWHM values are (0.2 and (0.1 eV, respectively. Different regions (A, B, C, D) are defined according to the observed evolution of KE and FWHM with RH.

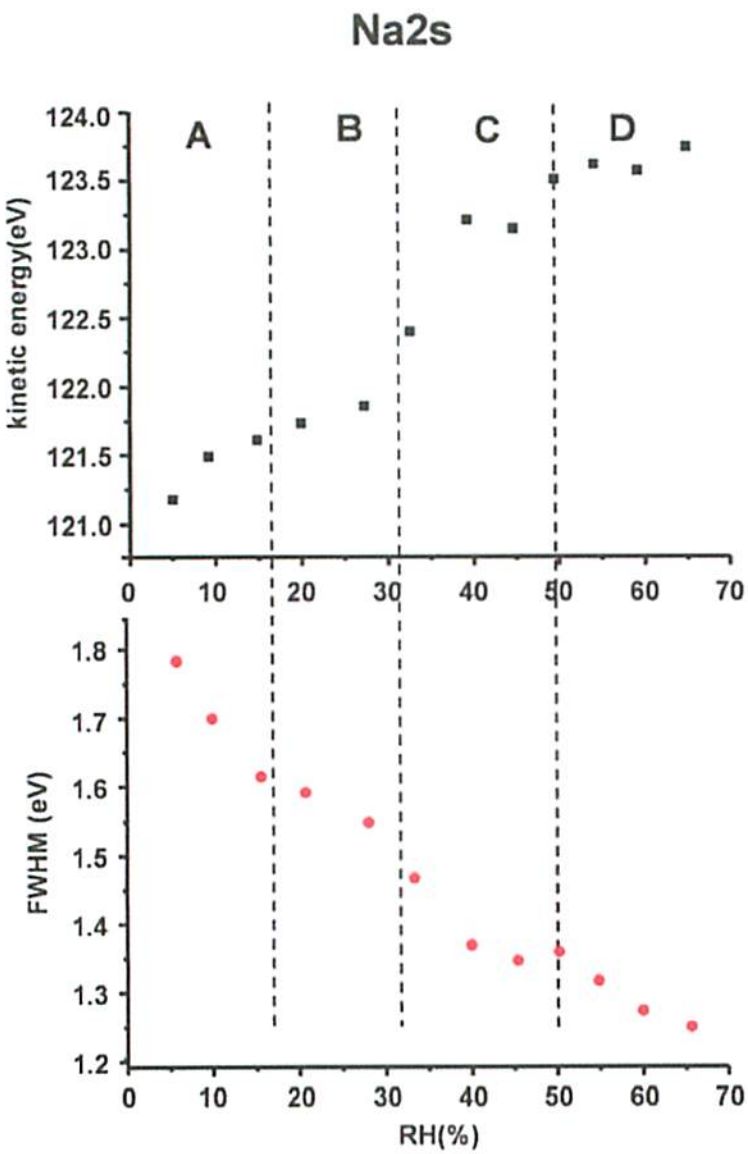

Figure 4. Kinetic energy (left) and surface oxygen content (right) vs relative humidity. The strong shift of the kinetic energy corresponds to a strong increase in the O 1s peak from adsorbed water. Adsorption of water triggers ions mobility on the surface and allows the discharging of the surface.